

Independent Joint Control of a 3-DOF Robotic System Using PI Controller

Sado F., Shahrul Na'im Sidek., Hazlina M. Yusuf

Department of Mechatronics Engineering,
International Islamic University Malaysia

P.O. Box 10, 50728, Kuala Lumpur, Malaysia.

e-mail: abdfsado1@gmail.com, {snaim, myhazlina@iium.edu.my}

Abstract— The use of robotic devices for repetitive exercising of patients with upper limb sensorimotor impairment has become accepted as effective in rehabilitation therapy. Two forms of rehabilitation robotic devices for upper limb are so far available which include the exoskeleton and end-effector based devices with the emphasis on proper joint coordination and control to actualize effective trajectory tracking and consequently effective therapy. An end-effector based 3 degree of freedom (3-DOF) rehabilitation platform is proposed in this work which uses brushless DC (BLDC) motor for actuation of the two revolute joints. For set-point and trajectory tracking of the revolute joints, each joint and corresponding link has been modeled has a SISO system and a PI compensator has been employed. Preliminary simulation studies showed the effectiveness of the proposed control framework.

Keywords—robotic; rehabilitation; sensorimotor; end-effector; compensator

I. INTRODUCTION

Recent studies have shown that over one million people suffer from stroke worldwide with about 0.79 million new or recurrent cases in US alone [1]. Two symptoms namely motor impairment and contracture have been identified to be associated with stroke patients which affect their activities of daily living (ADL). Several studies have however shown that repetitive exercising of the patient's affected limb and coaching by an expert therapist can significantly improve muscle plasticity and increase motor function of the limb to near regaining of the ADL [2-5].

In traditional rehabilitation therapy, a human therapist guides the impaired patient throughout the therapeutic process. This has a huge demand however on the therapist time and energy since the procedure requires repetitiveness and training over a long period of time. Thus, the use of robot therapist to assist patient in the rehabilitation exercises has become widely embraced. The key advantages of the robotic platforms have been identified to include an increase in therapy duration allowing more repetitions, objective quantification of patient's performance and a reduction in therapy cost [1, 2].

Many robotic devices for impaired patients' upper limb rehabilitation exist today [2-4] with different mechanical designs but two main classifications have been identified namely the end-effector and the exoskeleton based robotic devices. The end-effector types are designed to make only one point of contact with the patient [1] which is at the end-effector position (while the patients' elbow and shoulder are indirectly actuated as the platform moves in 3-D space),

whereas the exoskeleton based devices are designed to mimic the human arm [6] thus having the same number of degree of freedom (DOF) as the human arm. The main advantages of the end-effector based devices is their simplistic design and low cost whereas for the latter types, their main merit is that they allow a wide range of movement for the impaired limb and may also assist for measurements of other part of the arm. But a known disadvantages of this type is that they are usually more expensive and may be difficult to model and control since they have a high number of degrees of freedom. As far as clinical studies is concerned, however, the relative advantage of any one of these two types of devices to the other in terms of improving motor function has not been proven[2-4].

In this study, a portable end-effector based robotic device with 3DOF is proposed (two active revolute joints and one active prismatic joint). It is suggested that this device will complement the need of a therapist and allow patients to exercise in their homes. An important contribution is the use of brushless DC motors for actuation of the revolute joints. The advantages of the brushless DC (BLDC) motors is that they have a high power to weight ratio, high efficiency and reliability, high ripple-free torque, noiseless operation, low maintainability, and good dynamic control for variable speed applications which makes it suitable for rehabilitation robotics application.

The rest of the paper are organized as follows: section 2 describes the robot model of the proposed platform, section 3 gives the independent joint model for the two revolute joints and the last section is the result analysis.

II. ROBOT MODEL

A. Kinematic model

The proposed model of the rehabilitation robot consists of 3-active-DOF; two revolute joints and one prismatic joint. The revolute joints allows for the rehabilitation of the elbow and shoulder of the patients whereas the prismatic joint provides linear actuation for the end-effector.

The relationship between the individual joints of the rehabilitation device and the position and orientation of the robot's end-effector is expressed concisely by the four DH parameters given in Table I. The four parameters a_i , α_i , d_i , θ_i are generally known as the link length, link twist, link offset, and joint angle respectively [7].

TABLE I. DH PARAMETERS OF THE ROBOTIC DEVICE

Link	a_i	α_i	d_i	θ_i
1	0	0	0	θ_1^*
2	0	90	l	θ_2^*
3	l	0	d_3^*	0

The homogenous transformation matrix that relates the frame 3 to frame 0 obtained by using the parameters in the DH table is given by Equation (1) which forms the forward kinematic equation that represents the position and orientations of the end-effector frame or the wrist joint with respect to the fixed base frame.

$${}^0T_3 = \begin{bmatrix} c\theta_1 c\theta_2 & -c\theta_1 s\theta_2 & s\theta_1 & l(s\theta_1 + c\theta_1 c\theta_2) + d_3 s\theta_1 \\ c\theta_2 s\theta_1 & -s\theta_1 s\theta_2 & -c\theta_1 & l(c\theta_2 s\theta_1 - c\theta_1) - d_3 c\theta_1 \\ s\theta_2 & c\theta_2 & 1 & l s\theta_2 \\ 0 & 0 & 0 & 1 \end{bmatrix} \quad (1)$$

III. INDEPENDENT JOINT MODEL

A. The revolute joints

The two revolute joints of the robotic device for the elbow and shoulder rehabilitation are actuated by means of brushless DC motors. The choice of the brushless DC motor is informed by its high power to weight ratio, high efficiency and reliability, high ripple-free torque, noiseless operation, good dynamic control for variable speed applications [8, 9], and absence of brushes and commutator which reduce maintenance cost and increase motor life. To control each revolute joint, each link and the joint in question is modeled as a single-input/single-output system (SISO) actuated by the BLDC motor, see Fig. 2. Other attachments to the system are modelled as a load while the dynamic coupling among the joints is modeled as a disturbance to the SISO system. Since, the brushless DC motor is internally geared down by a ratio of 20 which is sufficient for rehabilitation task, no external gear reduction along the link is required.

B. Mathematical Model of DC motor Conventional

The mathematical model of a brushless DC motor is identical to that of a conventional DC motor except with some variations in the mechanical and electrical time constants [10]. This fact has been used in many literatures to derive the transfer function of the brushless DC motor from the mathematical model of the conventional type DC motor.

The differential equation for the armature current can be expressed as [7],

$$L \frac{di_a}{dt} + R i_a = V - K_b \omega_m \quad (2)$$

$$V_b = K_b \omega_m.$$

where V =armature voltage, L =armature inductance, R =armature resistance, V_b =back emf, K_b =back emf constant, i_a =armature current, ω_m = armature current.

In terms of the motor angular speed ω_m , the mechanical equation for the motor with inertia J , coefficient of friction B_m and load torque T_l can be written as,

$$J \frac{d\omega_m}{dt} + B_m \omega_m = K_m i_a - T_l \quad (3)$$

$$T_m = K_m i_a.$$

where T_m = generated torque, K_m = torque constant. Combining Equation (2) and (3), the transfer function for the DC motor system with $T_l=0$ can be derived as [7],

$$G(s) = \frac{\omega_m}{V} = \frac{K_m}{J_m L s^2 + (B_m L + J_m R) s + K_b K_m + B_m R} \quad (4)$$

Considering that the coefficient of friction is very small ($B_m \ll 1$) and making the following general assumptions for electro-mechanical systems [7, 11]:

1. $J_m R \gg B_m L$ (or $\frac{J_m}{B_m} \gg \frac{L}{R}$)
2. $K_b K_m \gg B_m R$

Equation (4) simplifies to

$$G(s) = \frac{\omega_m}{V} = \frac{K_m}{J_m L s^2 + J_m R s + K_b K_m} \quad (5)$$

and by re-arranging, we obtain

$$G(s) = \frac{\omega_m}{V} = \frac{\frac{1}{K_b}}{\frac{J_m R}{K_b K_m} s + \frac{J_m L}{K_b K_m} s^2 + 1} \quad (6)$$

From Equation (6), we obtain the mechanical time constant and the electrical time constant given by Equation (7) and (8) respectively

$$\tau_m = \frac{J_m R}{K_b K_m} \quad (7)$$

$$\tau_e = \frac{L}{R} \quad (8)$$

Equation (6) can therefore be written as

$$G(s) = \frac{\omega_m}{V} = \frac{\frac{1}{K_b}}{\tau_m \tau_e s^2 + \tau_m s + 1} \quad (9)$$

C. Mathematical Model of the Brushless DC motor system- the SISO system

The transfer function for the BLDC motor SISO system takes the same form of Equation (9) but the inductances (L) and the resistances (R) arrangements, and consequently the electrical and mechanical time constants differ significantly due to the introduction of phases and winding type [10, 11].

The mechanical and electrical time constant for the wye connected BLDC motor are given by (10) and (11) respectively [10].

$$\tau_m = \frac{J_{\Sigma R_{phase}}}{K_b (phase) K_m} \quad (10)$$

$$\tau_e = \frac{L_{l-l}}{\Sigma R_{phase}} \quad (11)$$

where

$$K_{b(phase)} = \frac{K_{b(l-l)}}{\sqrt{3}} \text{ (Motor voltage constant)} \quad (12)$$

K_m =motor torque constant

$R_{(l-l)}$ =motor resistance

$$\Sigma R_{phase} = 0.5 \Sigma R_{l-l} \quad (13)$$

$$\Sigma R_{l-l} = 1.35 R_{l-l} \quad (14)$$

$$K_{b(l-l)} = K_m \times 0.0605 \quad (15)$$

$L_{(l-l)}$ =motor inductance

J = the sum of motor armature inertia and reflected load inertia to the shaft.

By substitution of (12) and (13) into (10) and (11), the time constants can be written respectively

$$\begin{aligned} \tau_m &= \frac{\frac{\sqrt{3}}{2} J \Sigma R_{l-l}}{K_{b(l-l)} K_m} = (0.866) \frac{J \Sigma R_{l-l}}{K_{b(l-l)} K_m} \\ &= (1.169) \frac{J R_{l-l}}{K_{b(l-l)} K_m} \end{aligned} \quad (16)$$

$$\tau_e = \frac{2 L_{l-l}}{\Sigma R_{l-l}} = 1.481 \frac{L_{l-l}}{R_{l-l}} \quad (17)$$

The BLDC motor used for the revolute joints of the proposed rehabilitation robotic system is the BLEM512 GFS, 200VDC, with gear head of 1:20 from Oriental Motors Co. The parameters of the motor for the mathematical model are given in TABLE II.

The transfer function of the BLDC motor SISO system is therefore derived from Equation (9) by the use of the BLDC motor data plus some experimental measurement as follows:

$$\tau_m = (1.169) \frac{J R_{l-l}}{K_{b(l-l)} K_m} = 1.3 \text{ s}$$

where $J = 0.61 \times 10^{-4} \text{ Kg.m}^2$, $R_{l-l} = 10.5 \Omega$, $K_m = 90.9 \times 10^{-3} \text{ Nm/A}$, and

$$K_{b(l-l)} = 5.4 \times 10^{-3} \frac{\text{v-sec}}{\text{rad}}.$$

Also,

$$\tau_e = 1.481 \frac{L_{l-l}}{R_{l-l}} = 8.2 \times 10^{-3} \text{ s},$$

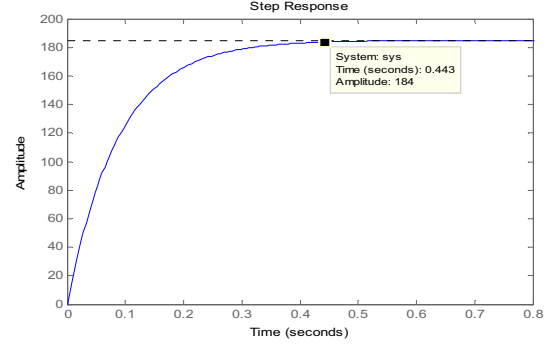
where $L_{l-l} = 0.058 \text{ H}$

Substituting for τ_e , τ_m and $K_{b(l-l)}$, the open loop transfer function for the BLDC motor system can be written as,

$$G(s) = \frac{\omega_m}{V} = \frac{185.2}{1.1 \times 10^{-4} s^2 + 1.3 s + 1} \quad (18)$$

The step response of the system with disturbance, $D = 0$ shows poor tracking of the reference input with settling time of 0.44s, zero overshoot and a steady state error of 1.2, see Fig. 1.

Fig. 1. Step response plot of the system



D. PWM speed control

The voltage input to the system is tuned by a PWM to analog voltage converter implemented as a second order low pass filter. This allows for the setting of the rotor speed by varying the duty cycle of the PWM signal from the microcontroller.

The transfer function for the second order low pass filter can be written as [12]

$$G(s) = \frac{\omega_m}{\text{duty}_{cycle}} = \frac{\omega_n^2}{s^2 + 2\zeta\omega_n s + \omega_n^2} \quad (19)$$

where

$$\omega_n = \frac{1}{\sqrt{(1 \times 10^3)^2 \times (1 \times 10^{-6})^2}} = \frac{1000 \text{ rad}}{s}$$

$$\zeta = \frac{3(1 \times 10^3 \times 1 \times 10^{-6})}{2\sqrt{(1 \times 10^3)^2 \times (1 \times 10^{-6})^2}} = 1.5$$

IV. SIMULATION RESULTS

A. Set-Point Tracking

To track a reference speed ω_m^d , the closed loop system is formed using a PI compensator as shown in Fig. 2. The control input $U(s)$ is given in the Laplace domain as [7]

$$U(s) = (K_p + \frac{K_I}{s})(\omega_m^d(s) - \omega_m - K_D s \omega_m) \quad (20)$$

where K_p , K_I are the proportional and integral gains respectively and K_D is set to zero. The overall closed loop transfer function using PI controller with the disturbance parameter $D=0$ is given as

$$G(s) = \frac{185.2(K_p s + K_I)}{1.1e-10s^4 + 1.63e-06s^3 + 0.004011s^2 + 1.303s + (1 + K_p s + K_I)} \quad (21)$$

The best performance of the SISO system is obtained after several heuristic tuning with $K_p = 0.62$, $K_i = 0.93$. In this case, there is no steady state error and no overshoot. The rise time and settling times are small at 0.018s and 0.03s respectively as shown in Fig. 3. This performance is quite sufficient for rehabilitation therapy.

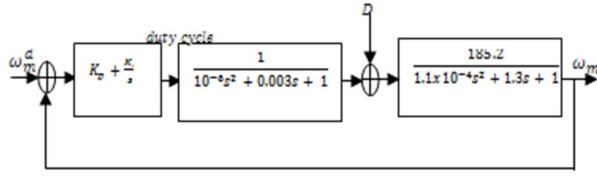


Fig. 2. The overall closed loop system using PI compensator

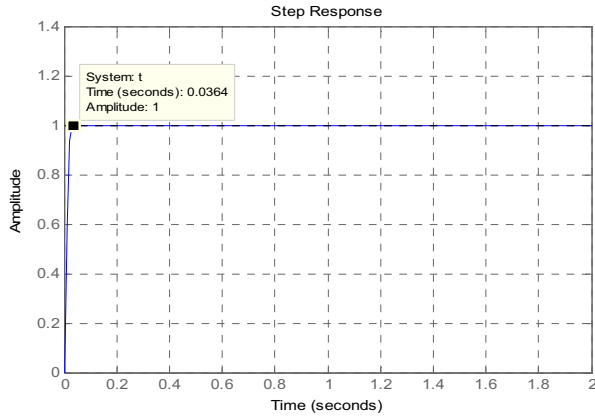


Fig. 3. Step response for $K_p = 0.62$, $K_i = 0.93$

B. Trajectory tracking

The Matlab/Simulink model of the single joint single link system (Fig. 2) trajectory tracking was developed and the system showed good tracking of reference speed as can be seen in Fig. 4. The actual speed is found to track the desired speed with a RMS error of 0.0876.

Fig. 5 shows the input disturbance rejection plot of the system obtained from the response plot of the actual speed to input disturbance transfer function. After 0.2s the input disturbance is found to decay by 86% which is quite adequate for the proposed application.

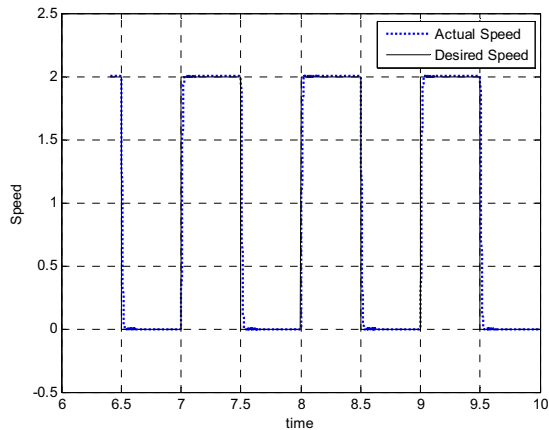


Fig. 4. Trajectory tracking

V. CONCLUSION

In this work an independent joint control of two revolute joints of a 3DOF rehabilitation robotic system using PI compensator has been presented. To control the joints, each of the joints and the corresponding link is model as a SISO system actuated by a BLDC motors. Simulation studies

showed that the proposed control framework is able to track the desired speed input to the actuator with a high degree of accuracy.

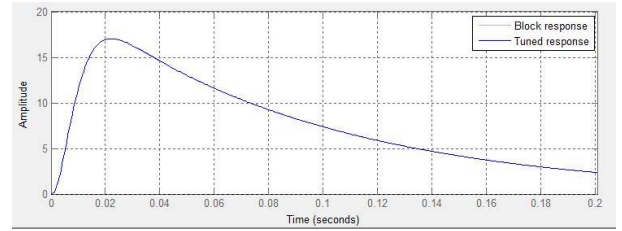


Fig. 5. Input Disturbance rejection

ACKNOWLEDGMENT

The work presented was carried out in the Biomechanics Research Laboratory of IIUM. The authors wish to gratefully acknowledge the grant funding from the Ministry of Higher Education Malaysia (RAGS12-002-0002).

REFERENCES

- [1] G. De Lee, W.-W. Wang, K.-W. Lee, S.-Y. Lin, L.-C. Fu, J.-S. Lai, et al., "Arm exoskeleton rehabilitation robot with assistive system for patient after stroke," in *Control, Automation and Systems (ICCAS), 2012 12th International Conference on*, 2012, pp. 1943-1948.
- [2] J. Eschweiler, K. Gerlach-Hahn, A. Jansen-Toy, and S. Leonhardt, "A survey on robotic devices for upper limb rehabilitation," *Journal of neuroengineering and rehabilitation*, vol. 11, p. 3, 2014.
- [3] L. Marchal-Crespo and D. J. Reinkensmeyer, "Review of control strategies for robotic movement training after neurologic injury," *Journal of neuroengineering and rehabilitation*, vol. 6, p. 20, 2009.
- [4] G. Kwakkel, B. J. Kollen, and H. I. Krebs, "Effects of robot-assisted therapy on upper limb recovery after stroke: a systematic review," *Neurorehabilitation and neural repair*, vol. 22, pp. 111-121, 2008.
- [5] C. Bütefisch, H. Hummelsheim, P. Denzler, and K.-H. Mauritz, "Repetitive training of isolated movements improves the outcome of motor rehabilitation of the centrally paretic hand," *Journal of the neurological sciences*, vol. 130, pp. 59-68, 1995.
- [6] J. Gunasekara, R. Gopura, T. Jayawardane, and S. Lalitharathne, "Control methodologies for upper limb exoskeleton robots," in *System Integration (SII), 2012 IEEE/SICE International Symposium on*, 2012, pp. 19-24.
- [7] M. W. Spong, S. Hutchinson, and M. Vidyasagar, *Robot modeling and control*: John Wiley & Sons New York, 2006.
- [8] S. Rambabu, "Modeling and control of a brushless DC motor," 2007.
- [9] A. Rao, Y. Obulesh, and C. Babu, "Mathematical modeling of bldc motor with closed loop speed control using pid controller under various loading conditions," *Journal of Engineering & Applied Sciences*, vol. 7, 2012.
- [10] G. Younkin, "Electric servo motor equations and time constants," Bulls Eye Marketing, Inc.
- [11] O. Oguntuyinbo, "PID control of brushless DC motor and robot trajectory planning simulation with MATLAB®/SIMULINK®," 2009.
- [12] D. M. Alter, "Using PWM output as a digital-to-analog converter on a TMS320F280X digital signal controller," Texas Instruments, Dallas, TX, Application Report SPAA88, 2006.